

basin boundaries, some basins overlap, and multiple agencies are involved in tracking and forecasting TCs. Compiling the activity over all seven TC basins, the 2011 season (2010/11 in the Southern Hemisphere) saw a well-below-average (1981–2010 base period) number of named storms (NS; wind speeds  $\geq 34$  kts or  $17.5 \text{ m s}^{-1}$ ) and hurricanes/typhoons/cyclones (HTC; wind speeds  $\geq 64$  kts or  $32.9 \text{ m s}^{-1}$ ) and an above-average number of major HTCs (wind speeds  $\geq 96$  kts or  $49.4 \text{ m s}^{-1}$ ). Globally, 74 named storms<sup>3</sup> developed during the 2011 season (global average is 89), with 38 becoming HTCs (global average is 44). Of these, 22 (compared to 26 in 2006, 18 in 2007, 20 in 2008, 16 in 2009, and 22 in 2010) attained major/intense status (global average is 19). Therefore, while the overall NS count was well-below average, the number of major/intense storms was above the IBTrACS global average.

On the whole, while global tropical cyclone activity was again below normal in 2011, it was higher than in 2010, which set the record for the lowest number of global TCs since the start of the satellite era. There were no clear-cut Category 5 systems during the year, an unusual occurrence, with the year's most intense systems: (1) Adrian, Dora, Eugene, Hilary, and Kenneth in the Northeast Pacific; (2) Ophelia in the North Atlantic; (3) Nanmadol, Songda, and Muifa in the Northwest Pacific; and (4) Yasi in the Australian region, all peaking at Category 4<sup>4</sup>.

The only basin which had substantially above-normal activity in 2011 was the North Atlantic, where elevated TC activity is a typical response to La Niña has been seen in 12 of the last 17 seasons since 1995. Conversely, the South Indian, North Indian, and

<sup>3</sup> It should be noted that in the Western North Pacific there were an additional seven unnamed tropical depressions recorded by the Japan Meteorological Agency (JMA) that were not included in this total.

<sup>4</sup> Typhoons Songda and Muifa were classified as Category 5 operationally by the Joint Typhoon Warning Center but Category 4 in the best-track dataset produced by Japan Meteorological Agency, the responsible World Meteorological Organization center for the Northwest Pacific.

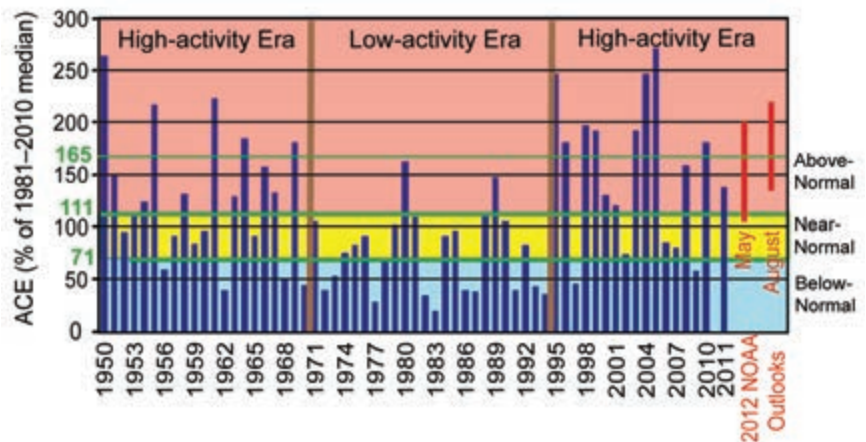


**Fig. 4.8. NOAA's ACE index expressed as percent of the 1981–2010 median value. ACE is calculated by summing the squares of the six-hourly maximum sustained wind speed (knots) for all periods while the storm has at least tropical storm strength. Red bars show NOAA's predicted ACE ranges in their May and August seasonal hurricane outlooks. Pink, yellow, and blue shadings correspond to NOAA's classifications for above-, near-, and below-normal seasons, respectively. The 165% threshold for a hyperactive season is indicated. Vertical brown lines separate high- and low-activity eras.**

Northeast Pacific basins experienced well-below-normal TC numbers (although the Northeast Pacific had an above-normal average number of hurricanes and major hurricanes). Part of the explanation for the low global number of tropical cyclones was that the characteristic La Niña boost to numbers in the Australian region, which would normally offset La Niña-induced deficits in many other hurricane regions, was absent in 2011, with both the Australian region and the Southwest Pacific basins experiencing near-normal activity.

2) ATLANTIC BASIN—G. D. Bell, E. S. Blake, C. W. Landsea, T. B. Kimberlain, S. B. Goldenberg, J. Schemm, and R. J. Pasch  
(i) 2011 Seasonal activity

The 2011 Atlantic hurricane season produced 19 tropical storms (TS), of which 7 became hurricanes and 4 became major hurricanes. The 30-year IBTrACS seasonal averages are 11.9 named storms, 6.4 hurricanes, and 2.7 major hurricanes (MH). The August–October (ASO) period is typically the peak of the season, and all but five named storms during 2011 formed in ASO.

The 2011 seasonal Accumulated Cyclone Energy (ACE) value (Bell et al. 2000) was  $126.3 \times 10^4 \text{ kt}^2$ , which corresponds to 137% of the 1981–2010 median (Fig. 4.8). NOAA classifies the 2011 season as above normal ([http://www.cpc.ncep.noaa.gov/products/outlooks/background\\_information.shtml](http://www.cpc.ncep.noaa.gov/products/outlooks/background_information.shtml)). This is the 12th above-normal season since the current high activity era for Atlantic hurricanes began in 1995

(Goldenberg et al. 2001), and the 14th busiest season since 1966. NOAA's seasonal hurricane outlooks, issued in late May and early August (<http://www.cpc.ncep.noaa.gov/products/outlooks/hurricane-archive.shtml>) by the CPC, indicated a high likelihood of an above-normal 2011 season (red bars).

Four global climate factors influenced the 2011 Atlantic hurricane season. Three of these contributed to more conducive conditions within the Main Development Region (MDR), including the active-Atlantic phase of the tropical multidecadal signal (sections 4d2vi and 4g of this report, and Bell and Chelliah 2006); La Niña (discussed in section 4b); and anomalously warm SSTs in the MDR (section 4d2iv). A fourth climate factor, the Indian Ocean dipole, may have acted to limit the overall activity for the 2011 season and is discussed in sections 4d2viii and 4h of this report.

*(ii) Storm tracks*

The Atlantic storm tracks during 2011 (Fig. 4.9, brown lines) were generally divided into three clusters. One cluster comprised six storms that formed over the central and eastern tropical Atlantic, which is the eastern half of the MDR (Fig. 4.9, green boxed region encompassing the tropical Atlantic Ocean and Caribbean Sea between 9.5°N and 21.5°N; Goldenberg et al. 2001). Five of these storms eventually became hurricanes (three became major) and three made landfall. Maria and Ophelia made landfall in Newfoundland, Canada, with tropical storm strength, and Irene made landfall as a hurricane along the US Atlantic coast.

The second cluster consisted of six systems (four named storms and two hurricanes, with one be-

coming Major Hurricane Rina) that formed over the western Caribbean Sea and Bay of Campeche, regions that often see increased activity during La Niña (e.g., 1989, 1996, and 2010). Five of these six systems made landfall as tropical storms, with only Don weakening to a tropical depression before moving over southeastern Texas. Arlene and Nate struck Mexico; Harvey made landfall in Belize and Mexico; Lee came ashore in south-central Louisiana, and Rina struck the Yucatan Peninsula.

The third cluster of tracks consisted of seven tropical storms that formed north of the MDR over the subtropical North Atlantic, and remained at sea throughout their life cycle (though Jose and Sean did pass close to Bermuda). This is one of the largest number of baroclinically-initiated (i.e., not from tropical waves) tropical storms since the satellite era began. On average, three to four named storms form over the subtropical North Atlantic per season and roughly two become hurricanes (McTaggart-Cowan et al. 2008; Kossin et al. 2010).

*(iii) Hurricane landfalls*

Irene was the first US hurricane landfall since 2008. This storm initially made US landfall in North Carolina (after making landfall in the Bahamas as a major hurricane), and then made another landfall as a tropical storm in New Jersey, subsequently causing major flooding in the Northeast. Irene was the most significant hurricane to strike the northeastern US since Hurricane Bob in 1991.

An analysis of the low US hurricane landfall frequency during 2009–11 (e.g., only one landfall in three seasons) was performed. The lack of landfalls during the below-normal 2009 season (Bell et al. 2010), and the occurrence of one landfall during the above-normal 2011 season, are consistent with past seasons of similar strength, although at the lower end of the distribution (Blake et al. 2011). However, the lack of hurricane landfalls during the hyperactive 2010 season (ACE > 165% of the median) is quite anomalous (Bell et al. 2011), as all previous hyperactive seasons had featured at least one US landfall, 92% had at least two landfalls, and 67% had at least three landfalls.

Two main atmospheric factors known to limit US hurricane landfalls were present during both 2010 and 2011: (1) a persistent mid-level trough and strong southwesterly flow over the western North Atlantic (Fig. 4.9) which steered all but one approaching hurricane (Irene) away from the US Atlantic coast; and (2) the absence of hurricanes either forming or

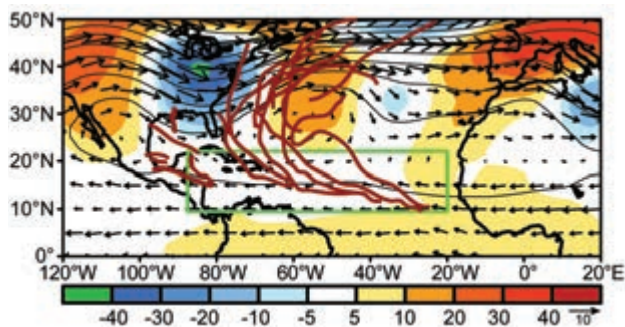


**FIG. 4.9. ASO 2011: 500-hPa heights (contours, m), anomalies (shading), and layer mean wind vectors (m s<sup>-1</sup>) between 600 hPa and 300 hPa. Atlantic named storm tracks are shown in brown. Green box denotes the MDR. Vector scale is below right of color bar. Anomalies are with respect to the 1981–2010 period monthly means.**

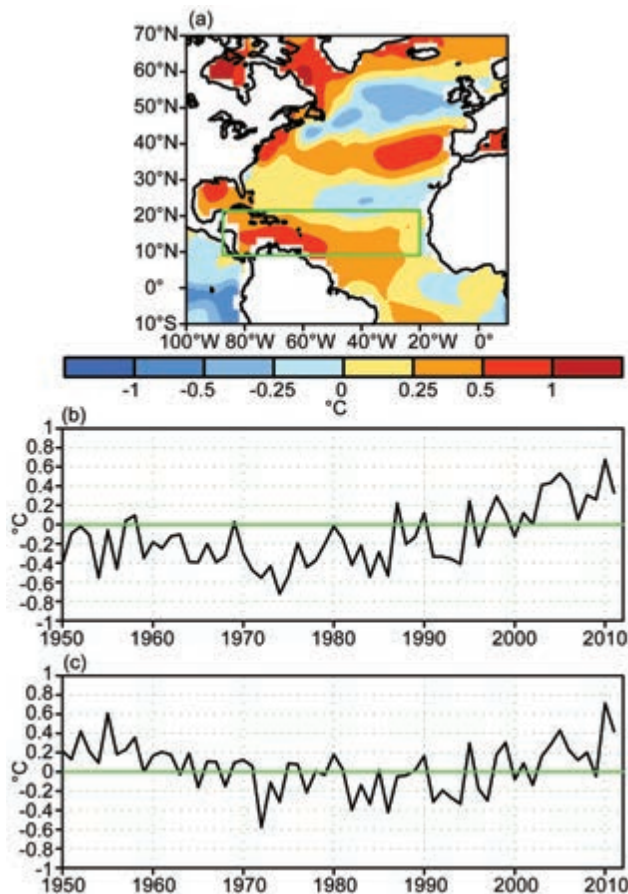


**FIG. 4.10.** (a) ASO 2011 SST anomalies ( $^{\circ}\text{C}$ ). (b) Time series of consecutive ASO area-averaged SST anomalies in the MDR [green box in (a)]. (c) Time series showing the difference between ASO area-averaged SST anomalies in the MDR and those for the entire global tropics ( $30^{\circ}\text{N}$ – $30^{\circ}\text{S}$ ). Anomalies are departures from the ERSST-v3b (Smith et al. 2008) 1981–2010 period monthly means.

propagating over the central and northern Gulf of Mexico. Historically, 50% of above-normal seasons have previously featured at least one hurricane formation in these regions. Also, such seasons often feature hurricanes that move into the central Gulf from the Caribbean Sea, yet none took such a track during either 2010 or 2011.

(iv) *Atlantic sea surface temperatures*

Sea surface temperatures (SST) in the MDR were above average during August–October 2011, with the largest departures (between  $+0.5^{\circ}\text{C}$  and  $+1.0^{\circ}\text{C}$ ) observed in the Caribbean Sea and western tropical North Atlantic (Fig 4.10a). The mean SST departure within the MDR was  $+0.33^{\circ}\text{C}$  (Fig 4.10b), which is  $+0.44^{\circ}\text{C}$  warmer than the average departure for the entire global tropics (Fig 4.10c). These conditions were partly responsible for the above-normal Atlantic hurricane season.

This anomalous warmth is related to weaker-than-average easterly trade winds (e.g., westerly anomalies) across the tropical Atlantic (Fig 4.11a). This combination of weaker trade winds and anomalously warm SSTs in the MDR (both of which typically become established prior to the start of the season) has generally prevailed since 1995 (Fig 4.11b) in association with the warm phase of the Atlantic Multidecadal Oscillation (AMO; Enfield and Mestas-Nuñez 1999) and the active Atlantic phase of the tropical multidecadal signal.

(v) *Atmospheric circulation*

The atmospheric circulation during ASO 2011 featured an interrelated set of conditions known to be exceptionally conducive for TC formation and inten-

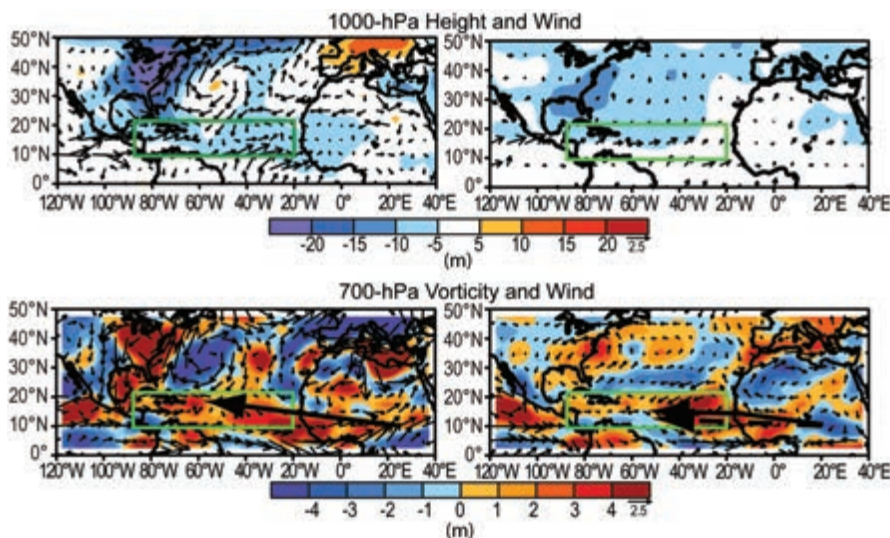


**FIG. 4.11.** (a) and (c) ASO 2011 anomalies and (b) and (d) difference between the 1995–2010 and 1971–1994 ASO means. Panels (a) and (b) show 1000-hPa heights (shading, m) and wind vectors ( $\text{m s}^{-1}$ ). Panels (c) and (d) show 700-hPa relative vorticity (shading,  $\times 10^{-6} \text{ s}^{-1}$ ) and wind vectors. In (c) thick arrow shows the axis of the African easterly jet (AEJ). In (d) thick solid (dashed) arrow indicates the mean position of the AEJ during 1995–2010 (1971–1994). Vector scales are below right of color bars. Green boxes denote the MDR. Anomalies are with respect to the 1981–2010 period monthly means.

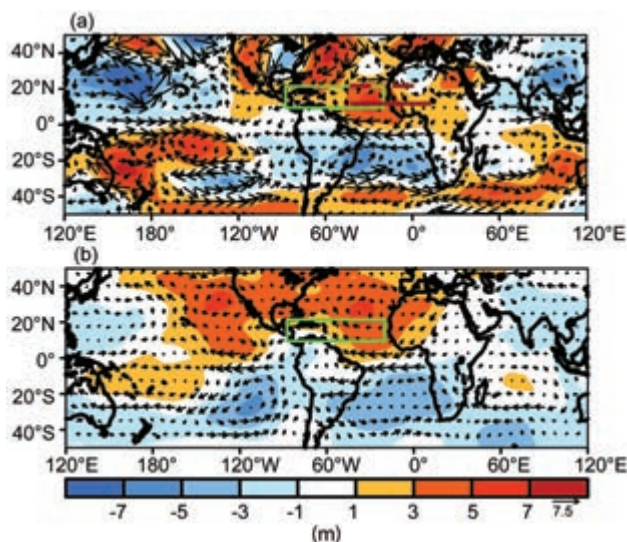


**FIG. 4.12.** 200-hPa streamfunction (shading,  $\times 10^6 \text{ m}^2 \text{ s}^{-1}$ ) and wind vectors ( $\text{m s}^{-1}$ ). (a) Anomalies during ASO 2011 and (b) difference between 1995–2010 and 1971–1994 ASO means. In (a) brown solid (dashed) line over the eastern MDR shows location of mean ridge axis during ASO 2011 (ASO 1995–2010). Anomalous ridges are indicated by positive values (red) in the NH and negative values (blue) in the SH. Anomalous troughs are indicated by negative values in the NH and positive values in the SH. Green boxes denote the MDR. Vector scale is below right of color bar. Anomalies are with respect to the 1981–2010 base period monthly means.

sification within the MDR (Landsea et al. 1998; Bell et al. 2011; Goldenberg et al. 2001; Bell and Chelliah 2006; Kossin and Vimont 2007). Ten tropical storms formed in the MDR this year, eventually producing six of the seven total hurricanes, all major hurricanes, and 88% of the seasonal ACE value.

In the lower atmosphere, ASO conditions within the MDR included weaker trade winds, a deep layer of anomalous cross-equatorial flow, and below-average 1000-hPa heights (Fig. 4.11a, blue shading). Across the Atlantic basin and sub-Saharan Africa, the low-level westerly anomalies extended above 700 hPa, the approximate level of the African Easterly jet (AEJ; Fig. 4.11c), and were associated with an anomalous  $2.5^\circ$ – $5^\circ$  latitude northward shift of the AEJ core (black arrow, Fig. 4.11c).

As a result, the bulk of the African easterly wave energy (Reed et al. 1977) was often centered well within the MDR. The AEJ also featured increased cyclonic shear along its equatorward flank (Fig. 4.11c, red shading), which dynamically favors stronger easterly waves. These conditions have generally prevailed since 1995, and are opposite to those seen during the low activity era of 1971–94 (Fig 4.11d).

Also during ASO 2011, anomalous easterly flow at 200 hPa extended from the Gulf of Guinea to the eastern North Pacific (Fig 4.12a), although this flow was less extensive than seen in 2010. This pattern reflected a stronger and more westward extension of the tropical easterly jet, and occurred in association with enhanced upper-level ridges that spanned the entire subtropical Atlantic in both hemispheres. This interhemispheric symmetry is another prominent feature of the current high activity era (Fig. 4.12b).

The above circulation anomalies resulted in weaker vertical wind shear (less than  $8 \text{ m s}^{-1}$ ) across the southern and western MDR (Fig 4.13), with the most anomalously weak shear located over the central tropical Atlantic and Caribbean Sea (Fig 4.13b). However, the area of anomalously weak shear was far less extensive than in 2010.

These conditions were part of the larger-scale pattern that included increased shear over both the eastern equatorial Atlantic and the eastern tropical North Pacific (Fig. 4.13b, blue shading), and are typical of other above-normal seasons since 1995 (Bell and Chelliah 2006; Bell et al. 2011). There was also an area of weaker-than-average shear over the northwestern Atlantic near Bermuda during ASO 2011, which could have helped promote the high number of named storms that formed in the subtropics.

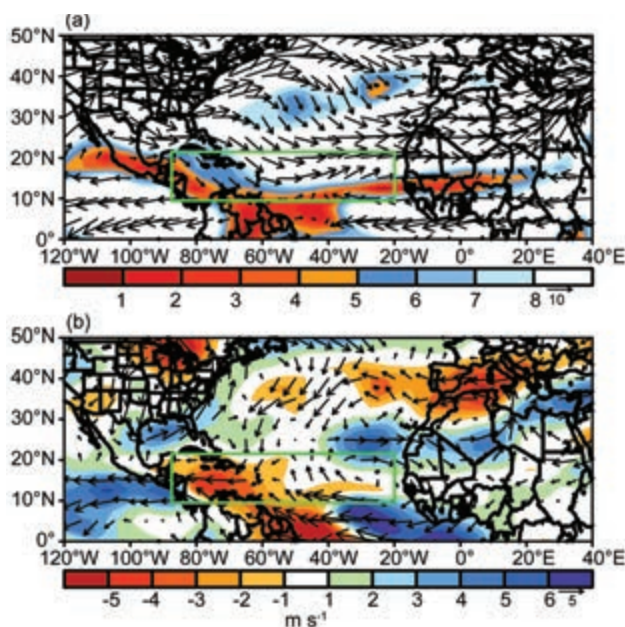


**FIG. 4.13.** ASO 2011 vertical wind shear magnitudes and vectors ( $\text{m s}^{-1}$ ): (a) total and (b) anomalies. Green boxes denote the MDR. Vector scales are below right of color bars. Anomalies are with respect to the 1981–2010 period monthly means.

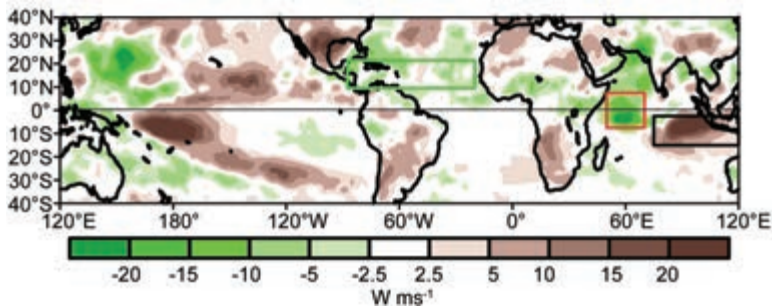


**FIG. 4.14. ASO 2011 anomalous outgoing longwave radiation (OLR,  $W m^{-2}$ ). Red (black) box denotes the western (eastern) portion of the Indian Ocean dipole (IOD). Green box denotes the MDR. Anomalies are with respect to the 1981–2010 period monthly means.**

These circulation anomalies were accompanied by a stronger Atlantic ITCZ and enhanced convection across the MDR (Fig. 4.14). They were also associated with an enhanced West African monsoon system, as indicated by enhanced convection across the African Sahel and Sudan regions and by a large area of negative velocity potential anomalies over northern Africa (Fig. 4.15a). Similar anomaly patterns have been present throughout the current high activity era (Fig. 4.15b).

For the Atlantic basin, the above conditions meant that many tropical storms formed within the MDR, primarily from easterly waves moving westward from Africa. These systems entered an extensive area of below-average pressure, deep tropical moisture, increased low-level convergence, and increased cyclonic shear south of the AEJ core-conditions known to be conducive for tropical cyclone formation. Many of these systems then generally strengthened while propagating westward within the extended region of weak vertical wind shear and anomalously warm SSTs.

*(vi) The tropical multidecadal signal*

Since 1995, more than 70% (12 of 17) of Atlantic hurricane seasons have been above normal, and only 2 have been below normal (Fig. 4.8). This elevated level of activity contrasts sharply with the 1971–94 low-activity era, when one-half of seasons were below normal and only three were above normal.

The sharp transition to the current high activity era reflected a phase change in the tropical multidecadal signal. This signal includes the leading modes of tropical convective rainfall variability and Atlantic SSTs occurring on multidecadal time scales (Bell and Chelliah 2006; Bell et al. 2007). It directly links atmospheric variability across the central and eastern MDR to multidecadal fluctuations in the strength of the West African monsoon system (Landsea and

Gray 1992; Landsea et al. 1998; Bell et al. 2009; Goldenberg and Shapiro 1996; Goldenberg et al. 2001; Bell and Chelliah 2006; Kossin and Vimont 2007).

Between 1994 and 1995, the ocean-atmosphere system switched to the active Atlantic phase of the tropical multidecadal signal, which features an enhanced West African monsoon system (Fig. 4.15b) and above-average SSTs in the MDR (i.e., the warm phase of the AMO; Fig. 4.10). As a result, the atmospheric circulation within the MDR

became much more conducive to Atlantic hurricane activity in 1995, as also indicated by the transition to weaker vertical wind shear (Fig. 4.16a), weaker 700-hPa zonal winds (Fig. 4.16b), and cyclonic (rather than anticyclonic) relative vorticity at 700 hPa across the southern MDR (Fig. 4.16c).

*(vii) Indian Ocean dipole*

The Indian Ocean dipole (IOD) reflects opposite patterns of anomalous tropical convection between the western and eastern Indian Ocean (Saji et al. 1999; Saji and Yamagata 2003a,b). A strong positive phase of the IOD was present during ASO 2011 (Fig. 4.17a), as indicated by enhanced convection over the western equatorial Indian Ocean and suppressed convection

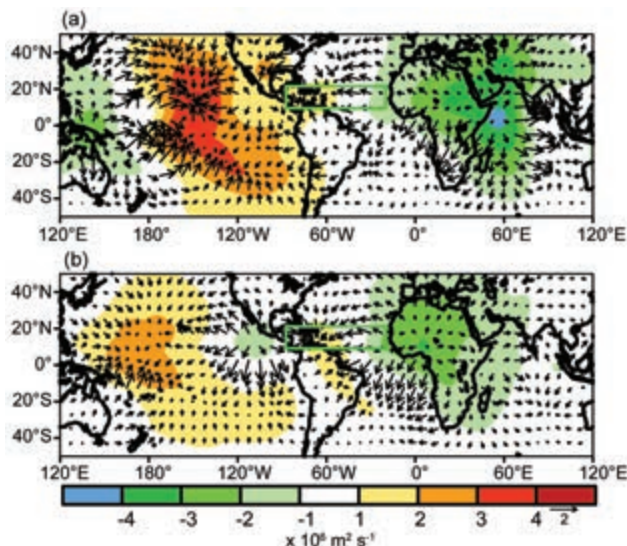


**FIG. 4.15. 200-hPa velocity potential (shading,  $\times 10^6 m^2 s^{-1}$ ) and divergent wind vectors ( $m s^{-1}$ ): (a) ASO 2011 anomalies and (b) difference between the 1995–2010 and 1971–94 ASO means. Green boxes denote the MDR. Vector scale is below right of color bar. Departures are with respect to the 1981–2010 period monthly means.**

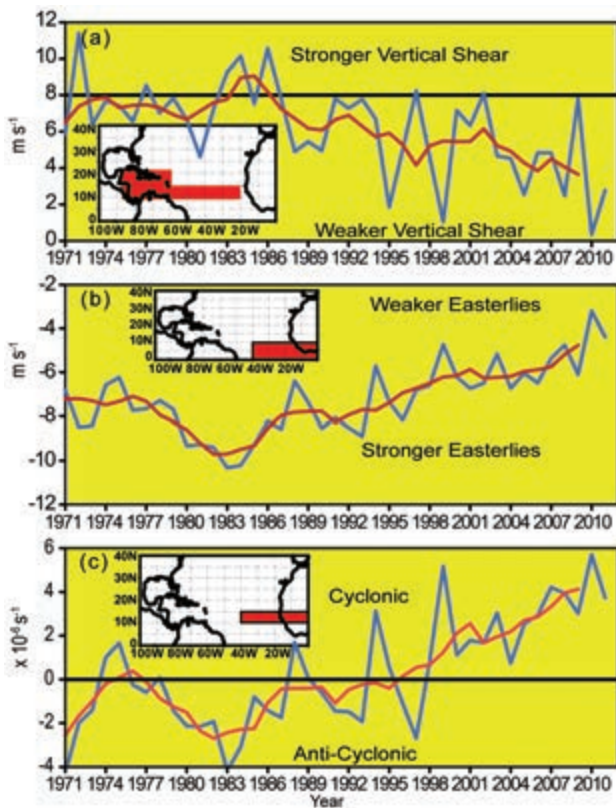


**FIG. 4.16.** Time series showing consecutive ASO values of area-averaged (a) 200-hPa–850-hPa vertical shear of the zonal wind ( $m s^{-1}$ ), (b) 700-hPa zonal wind ( $m s^{-1}$ ) and (c) 700-hPa relative vorticity ( $\times 10^{-6} s^{-1}$ ). Blue line shows unsmoothed values and red line shows a five-point running mean of the time series. Averaging regions are shown in the insets.

over the eastern tropical Indian Ocean (Fig. 4.14, red and black boxes, respectively).

There have been eight significant positive IOD events since reliable global outgoing longwave radiation (OLR) data became available in 1979. Figure 4.17b shows the Atlantic hurricane activity for these eight seasons. While these events have occurred during all phases of ENSO, they are typically associated with reduced Atlantic hurricane activity. The positive IOD event in 2011 may have been one reason why the overall Atlantic activity was lower (i.e., at the low end of the NOAA seasonal outlook issued in August, see Fig. 4.8) than what might have been expected given the combination of conducive climate factors present.

Specifically, the observations suggest that the IOD may have acted to limit the 2011 Atlantic hurricane activity by weakening both the West African monsoon circulation and the La Niña-related convection patterns. There are three indications of a weaker West African monsoon system compared to the 1995–2010 mean. First, the anomalous upper-level divergent cir-

ulation over northern Africa was weaker and less focused, and the anomalies were actually less than those over the western equatorial Indian Ocean (Fig. 4.15a). Second, the position of the 200-hPa subtropical ridge axis over the eastern MDR was located approximately  $10^\circ$  latitude farther south than the 1995–2010 mean (red lines, Fig. 4.12a). A similar southward shift of the ridge axis was seen during the 2007 Atlantic hurricane season, which also featured a strong positive IOD (Bell et al. 2008). Third, the anomalous southerly flow in the lower atmosphere was confined to the southern MDR and Gulf of Guinea region, rather than extending well into the central MDR and the African Sahel region (Fig. 4.11a).

The positive IOD also appears to have affected the La Niña-related convection patterns. One component of La Niña is an extensive area of enhanced convection across Indonesia and the eastern Indian Ocean. However, convection was suppressed over the eastern

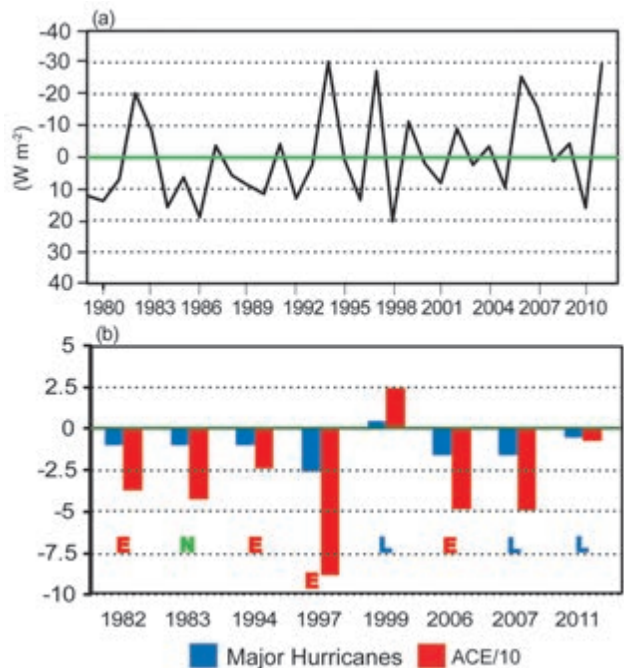


**FIG. 4.17.** (a) ASO time series of the IOD, calculated as the difference in area-averaged OLR anomalies ( $W m^{-2}$ ) between the western and eastern Indian Ocean (western minus eastern; boxes shown in Fig. 4.14). Anomalies are with respect to the 1981–2010 base period. (b) Anomalous Atlantic major hurricane (blue) and ACE/10 (i.e.,  $\times 10^3 kt^2$ ) activity associated with storms first named in the MDR when there was a strong positive IOD during ASO. Anomalies for years during 1979–1994 (low-activity era) and 1995–2011 (high-activity era) are based on the respective period means. Corresponding El Niño (red E), La Niña (blue L), and ENSO-neutral (green N) periods are indicated.

Indian Ocean during ASO 2011 in association with the positive IOD (Fig. 4.15), meaning that the La Niña forcing onto the atmospheric circulation was weaker than if no IOD signal had been present. A similar observation was made by Bell et al. (2008) for the 2007 Atlantic hurricane season.

3) EASTERN NORTH PACIFIC BASIN—M. C. Kruk, C. J. Schreck, and P. A. Hennon

(i) Seasonal activity

The Eastern North Pacific (ENP) basin is officially split into two separate regions for the issuance of warnings and advisories by NOAA's National Weather Service. NOAA's National Hurricane Center (NHC) is responsible for issuing warnings in the eastern part of the basin that extends from the Pacific Coast of North America to 140°W, while NOAA's Central Pacific Hurricane Center (CPHC) in Honolulu, Hawaii, is responsible for issuing warnings in the Central North Pacific region between 140°W and the date line. In this section, analysis summarizing the tropical cyclone (TC) activity in both these warning areas will be presented using combined statistics, along with information specifically addressing the observed activity and impacts in the Central North Pacific (CNP) region.

The ENP hurricane season officially spans from 15 May to 30 November, although storms can develop outside of the official season, especially during El Niño events. Hurricane and TC activity in the eastern area of the basin typically peaks in September, while in the central Pacific TC activity normally reaches its seasonal peak in August (Blake et al. 2009).

Only 11 named storms (NSs) formed in the ENP during 2011 and none formed in the CNP (Fig. 4.17). The 1981–2010 IBTrACS seasonal averages for the basin are 16.7 NSs, 8.9 hurricanes, and 4.3 major hurricanes. While the 2011 numbers are below average, all but one of the NSs (TS Fernanda) strengthened to at least hurricane status. The number of resulting hurricanes (10) and major hurricanes (6) were actually both above average. Five of the six major hurricanes even reached Category 4 status. This was the first time since records began in 1949 that more than 90% of the NSs became hurricanes and more than 50% also became major hurricanes. Despite the large fraction of strong storms, the ACE index for 2011 was  $121.8 \times 10^4 \text{ kt}^2$  (Fig. 4.18), which is below the 1981–2010 mean of  $144.0 \times 10^4 \text{ kt}^2$  (Bell et al. 2000; Bell and Chelliah 2006).

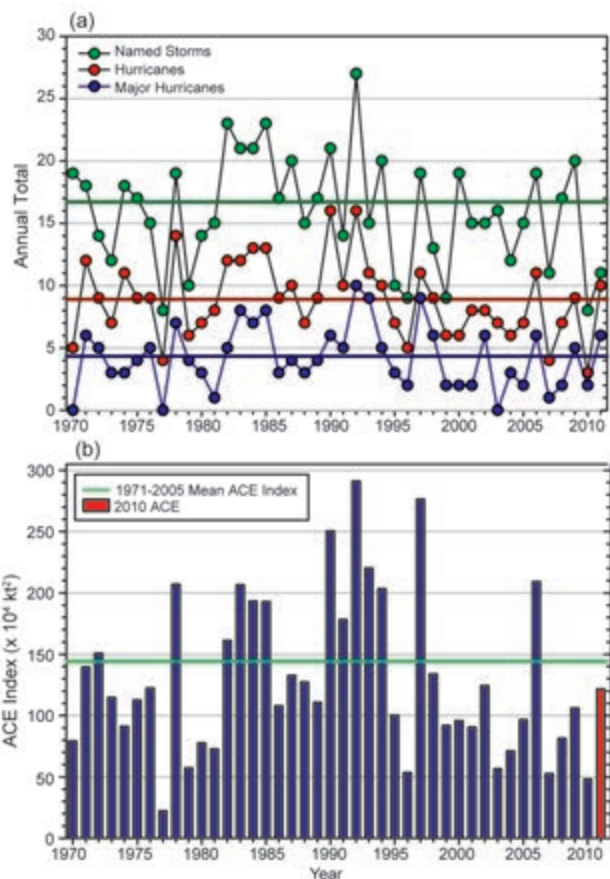


**FIG. 4.18. Seasonal TC statistics for the ENP basin over the period 1970–2011: (a) number of named storms, hurricanes, and major hurricanes, and (b) the ACE index with the seasonal total of 2011 highlighted in red. The time series shown includes the corresponding 1981–2010 base period means for each parameter.**

(ii) Environmental influences on the 2011 season

Figure 4.19 illustrates the background conditions for TC activity in the ENP during 2011. The overall patterns were dominated by La Niña. Sea surface temperatures (SSTs) were below normal over most of the ENP (Fig. 4.19a) and positive outgoing longwave radiation (OLR) anomalies (Fig. 4.19b, warm colors) suggest that convection was suppressed in the ITCZ. Enhanced vertical wind shear existed over most of the basin (Fig. 4.19c). Each of these factors acted to suppress TC activity, particularly in the ITCZ. Conditions were somewhat more favorable along the Central American coastline. Enhanced convection was observed along the coast (Fig. 4.19b, cool colors) and the SST anomalies were less negative in that area. Consistent with these patterns, most of the TCs did form near the coast.

Although conditions over the ENP were generally unfavorable for TCs during 2011, Fig. 4.19d shows 850-hPa westerly wind anomalies over the basin.